Journal of Materials Chemistry C

ROYAL SOCIETY OF CHEMISTRY

PAPER

View Article Online
View Journal | View Issue

Cite this: J. Mater. Chem. C, 2023, 11, 15030

Electrical conductivity and DFT investigations of a 2D Cu^{I}-$TCNQ^{II-}$ framework†

Ashley L. Sutton, Brendan F. Abrahams,* Christopher J. Commons, A. David Dharma, Lars Goerigk, Simon G. Hardin, Timothy A. Hudson and Richard Robson

Received 7th September 2023,
Accepted 13th October 2023

DOI: 10.1039/d3tc03237j

rsc.li/materials-c

An investigation of the coordination polymer, $[Cu_2(Me_2pz)(TCNQ)]$ (Me_2pz = 2,5-dimethylpyrazine) is described. The structure of $[Cu_2(Me_2pz)(TCNQ)]$ is comprised of 2D sheets with mean plane sheet-to-sheet separations closer than that of graphene sheets in graphite. Electrical conductivity measurements on the framework indicate semiconductor behaviour with a σ_{300K} = 9.8 × 10^{-8} S cm^{-1} and an E_a = 0.43(3) eV. Density functional theory studies reveal a band structure comprised predominatly by donor TCNQ and acceptor Me_2pz ligand-p oribtals. This investigation also resulted in the formation of Cu(TCNQ) (phase I) from the reaction mixture that yielded $[Cu_2(TCNQ)(Me_2pz)]$. A redetermination of the crystal structure of Cu(TCNQ) is reported.

Introduction

In recent years, there has been considerable effort to improve the charge-transport properties of porous coordination polymers.[1,2] Some of the most prominent and highly conductive systems have been planar or near-planar 2D frameworks. These include $[Ni_3(BHT)_2]$ (H_6BHT = benzenehexathiol), and $(Me_2NH_2)_2[Fe_2(can)_3]$ (H_2can = chloranilic acid), which have room temperature conductivities of 0.15 S cm^{-1} and 1.4 × 10^{-2} S cm^{-1} respectively.[3,4] The high electrical conductivity of each material is attributed to ligand mixed valency.

7,7,8,8-Tetracyanoquinodimethane, TCNQ, has attracted significant attention as a mixed-valent partner in organic charge-transfer complexes.[5] Perhaps one of the most prominent examples of charge transfer complexes is tetrathiafulvalene-7,7,8,8-tetracyanoquinodimethane, TTF-TCNQ, which displays metallic conductivity (>10^5 S cm^{-1} at 58 K).[6] Three accessible oxidation states of TCNQ exist, which leads to a considerable potential for mixed valency. The neutral form of TCNQ is a strong π acceptor, while the radical monoanion, which may be accessed through a one electron reduction, can be considered a weak π-donor. A second one electron reduction leads to the formation of the dianion which is a strong π donor (Fig. 1). Although the dianion is susceptible to air oxidation it can be stabilised by coordination to metal centres and through its participation in charge transfer interactions with π-acceptors.[7–18]

Not surprisingly, given that each of the nitrile groups has the potential to act as a donor group, there has been long-term interest in metal-TCNQ materials. Cu(TCNQ) has been the focus of particular attention, as its semi-conducting properties depend upon the method of preparation. Variability in the electrical conductivity of Cu(TCNQ) was explained by Dunbar and co-workers who discovered that Cu(TCNQ) existed in two structural forms, a kinetic product (phase I) and a thermodynamic product (phase II).[19] Both phases act as semiconductors with phase I offering superior electrical conductivity.

As part of the general interest in metal complexes of TCNQ, we have directed our efforts towards the generation of $TCNQ^{2-}$ coordination polymers.[7–16] As part of an investigation into $Cu^{I}_2(TCNQ^{-II})$ and $Cu^{I}_2(F_4TCNQ^{-II})$ coordination polymers we reported the synthesis and structure of $[Cu_2(Me_2pz)(TCNQ)]$ (Me_2pz = 2,5-dimethylpyrazine).[14] This 2D framework displayed structural features that warranted further attention. In

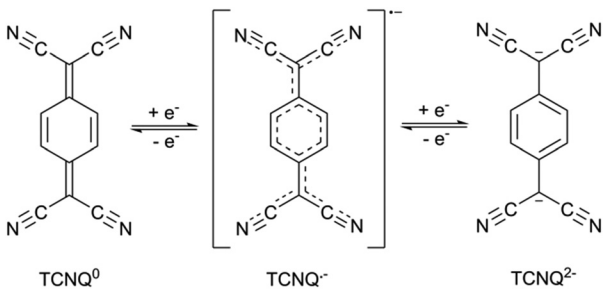

Fig. 1 Oxidation states of TCNQ.

School of Chemistry, University of Melbourne, Victoria, 3010, Australia.
E-mail: bfa@unimelb.edu.au; Tel: +61 3 8344 0341

† Electronic supplementary information (ESI) available: Details of Kistenmacher relationship calculations, electrical conductivity and computational details. CCDC 2291474. For ESI and crystallographic data in CIF or other electronic format see DOI: https://doi.org/10.1039/d3tc03237j

particular, it is noted that the mean planes of the 2D sheets are separated by a distance of 3.20 Å which is shorter than the separation of graphene sheets in graphite (3.41 Å).[20] Given the ability of TCNQ to act as a mixed-valent species, we have further explored physical properties of $[Cu_2(Me_2pz)(TCNQ)]$ which are reported herein. This investigation is complemented by density functional theory (DFT) calculations which provide insight into electrical conductivity pathways.

Results and discussion

The structure of $[Cu_2(Me_2pz)(TCNQ)]$, is comprised of crystallographically equivalent trigonal planar copper(I) centres, which are coordinated by two $TCNQ^{2-}$ anions and one Me_2pz ligand.[14] Each $TCNQ^{2-}$ anion coordinates four copper centres at the corners of a rectangle to form a $[Cu_2(TCNQ)]$ sheet. The remaining copper(I) sites are occupied by bridging Me_2pz ligands (Fig. 2). Whilst the Me_2pz ligand is co-planar with the mean plane of the sheet, the aromatic core of the $TCNQ^{2-}$ is rotated from the mean plane by approximately 13°. Sheets stack parallel to the [4 0 1] direction. Face-to-face interactions between Me_2pz and $TCNQ^{2-}$ ligands of neighbouring sheets, results in the generation of infinite π–π stacks (Fig. 3). This stacking of the 2D $[Cu_2(Me_2pz)(TCNQ)]$ networks results in an intersheet Cu···Cu separation of 3.20 Å.

Replacement of Me_2pz with the chelating ligand *N*, *N*′-tetramethyl-ethylenediamine (Me_4en) yields a very similar 2D framework with composition $[Cu_2(TCNQ)(Me_4en)_2]$, whilst 2-aminopyrazine yields an open 3D framework.[14] Clearly the type of co-ligand used can have a considerable impact on the dimensionality of the polymeric material.

Charge-transfer interactions commonly occur in X_4TCNQ^{2-} (X = H or F) based compounds and in certain instances result in unusual and interesting properties.[15–18] The degree of charge transfer can be estimated by various methods[5,21–24] that are commonly linked to an estimation of the of the charge (q) of the

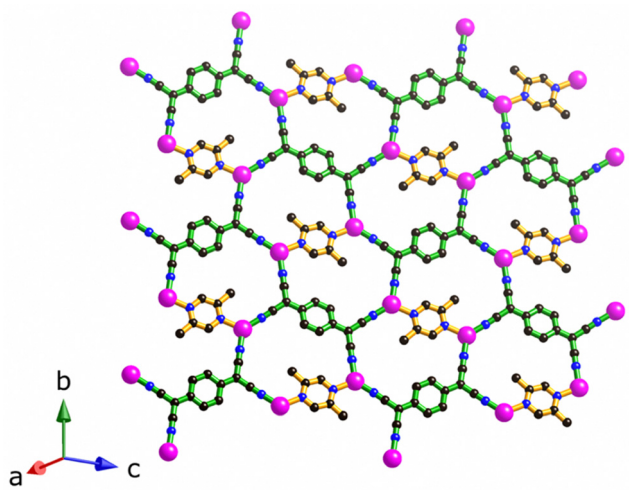

Fig. 2 The 2D sheet structure of $[Cu_2(Me_2pz)(TCNQ)]$; carbon, nitrogen and copper atoms in black, blue and pink respectively.

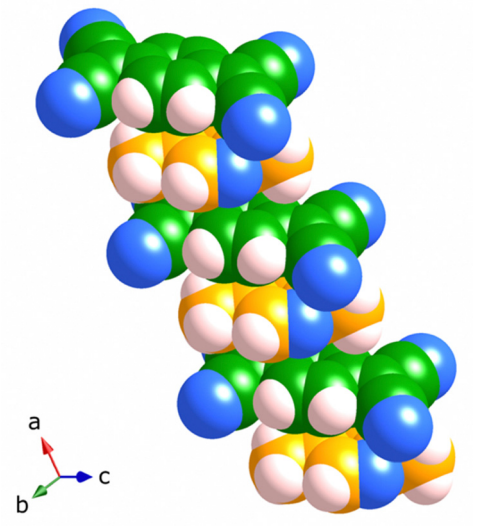

Fig. 3 Space-filling representation of $TCNQ^{2-}$ (green carbon atoms) and Me_2pz (yellow carbon atoms) ligands from adjacent $[Cu_2(Me_2pz)(TCNQ)]$ sheets. Nitrogen atoms in blue and hydrogen atoms in pale pink.

TCNQ species. The Kistenmacher equation is an empirical relationship represented by the formula:

$$q = A[c/(b + d)] + B$$

where b, c and d are bond lengths and A and B are constants (see ESI†).[21] The Kistenmacher relationship for the TCNQ species within the $[Cu_2(Me_2pz)(TCNQ)]$ framework yields a $q = -2.01(14)$ consistent with the retention of the dianionic form of the TCNQ (see ESI†) in the formation of the coordination polymer.

The short sheet-to-sheet separation and the infinite mixed-stacks of Me_2pz and $TCNQ^{2-}$ prompted an examination of the electrical conductivity of $[Cu_2(Me_2pz)(TCNQ)]$. Although many X_4TCNQ^{2-} coordination polymers have been reported,[15] there have been relatively few conductivity studies.[16,25] In this current work two-point pressed-pellet conductivity measurements reveal a value of $\sigma = 9.8 \times 10^{-8}$ S cm^{-1} at 300 K. Variable temperature measurements between 250 and 300 K, show an increase in conductivity with temperature, indicating semiconductor behaviour. Current density-electric field strength plots for $[Cu_2(Me_2pz)(TCNQ)]$ are presented in Fig. S2.1 (ESI†). Through application of the Arrhenius model, an estimation of the activation energy (E_a) of 0.43(3) eV was determined (Fig. 4).

With such significant π–π interactions it is somewhat surprising the charge-transport is not greater, especially given that non-TCNQ frameworks, albeit those utilising TTF-type ligands, have displayed considerable through-space charge-transport.[26,27]

The electronic band structure of $[Cu_2(Me_2pz)(TCNQ)]$ has been examined using solid-state DFT. The calculated band structure and density of states plots at the HSE06[28]//PBE[29]-D3(BJ)[30,31] level of theory are presented in Fig. 5. The conduction and valence bands of the $[Cu_2(Me_2pz)(TCNQ)]$ framework are comprised predominantly of ligand *p* orbitals

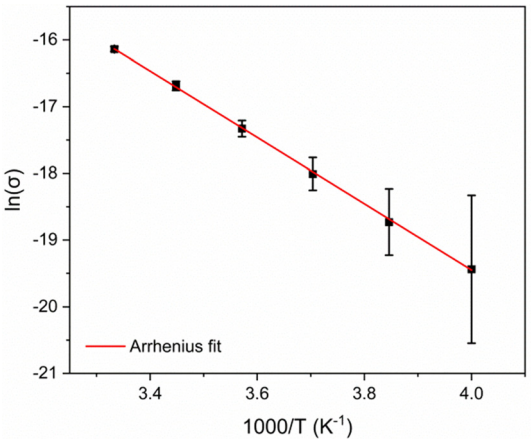

Fig. 4 Arrhenius plot for the $[Cu_2(Me_2pz)(TCNQ)]$ compound.

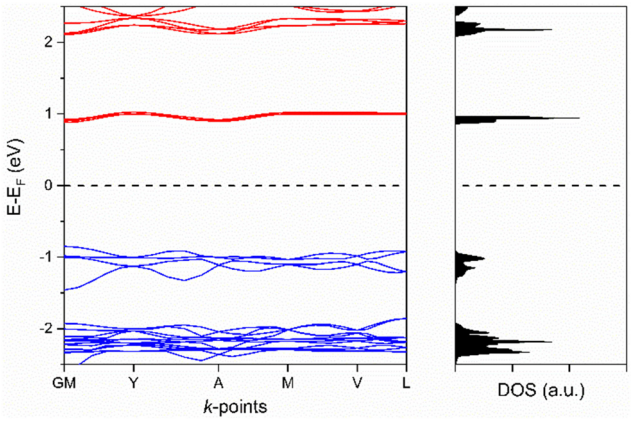

Fig. 5 Band structure and density of states (DOS) for $[Cu_2(Me_2pz)(TCNQ)]$. The valence and conduction bands are shown in blue and red respectively.

from the Me_2pz and $TCNQ^{2-}$ respectively (see ESI,† Fig. S3.1). This is unsurprising, given the mixed stack packing arrangement of $TCNQ^{2-}$ and Me_2pz. As expected, Me_2pz ligands act as the acceptor whilst the $TCNQ^{2-}$ ligands serve as donors. The calculated electronic bandgap of 1.7 eV, effectively represents the difference between the ionisation energy of the donor ($TCNQ^{2-}$) and the electron affinity of the acceptor (Me_2pz). There is a very minor contribution from the Cu-d orbitals to the valence band which alters the valence energy, although such a small contribution is unlikely to indicate metal–ligand mediated charge-transport.

The conduction and valence band dispersions are moderate for a coordination polymer at 190 and 120 meV respectively. The largest dispersion in the conduction band occurs along the G–Y vector in reciprocal space, which corresponds to a vector along stacks of the Me_2pz ligands. We note it may be possible to generate a framework with enhanced semiconductor behaviour through the use of a ligand with a comparable geometric profile to Me_2pz but with a higher electron affinity and high degree of charge delocalisation.

A final interesting aspect of this work relates to the air oxidation of the sample that occurs if the crystals of $[Cu_2(Me_2pz)(TCNQ)]$ remain in the mother liquor. Over a period of days the orange $[Cu_2(Me_2pz)(TCNQ)]$ crystals are accompanied by black, phase I Cu(TCNQ) crystals which were suitable for X-ray crystallography. It would appear that precautions to exclude atmospheric oxygen failed to prevent the slow oxidation of the TCNQ dianion to the radical monoanionic form. It was uncertain as to whether the Cu(TCNQ) crystals formed from the orange $[Cu_2(Me_2pz)(TCNQ)]$ crystals or grew independently from the mother liquor. When less stringent conditions relating to exclusion of air are employed, the orange $[Cu_2(Me_2pz)(TCNQ)]$ crystals are accompanied by crystals of Cu(TCNQ) which form at the same time, suggesting that Cu(TCNQ) is formed directly from the mother liquor. The original structure determination of the phase I crystals was hampered by the quality of the crystals, which were produced by mixing either TCNQ or $TCNQ^-$ with Cu(I) in acetonitrile.[19] The crystallographic problems included severe disorder and significant pseudomerohedral twinning. The original crystal structure was reported with cell dimensions $a = b = 11.266(2)$ Å, $c = 3.8878(8)$ Å, $\alpha = \beta = \gamma = 90^\circ$. Although the cell dimensions were consistent with a tetragonal cell, a satisfactory refinement in tetragonal symmetry could not be achieved because of the poor quality of the crystalline product. The structure was ultimately solved and refined in the monoclinic space group, *Pn*, using isotropic displacement parameters. The R_1 and wR_2 values of 23.2 and 48.1% reflect the poor quality of the crystals. The Cu(TCNQ) crystals obtained from oxidation of $TCNQ^{2-}$, as reported in this current work, were examined using X-ray crystallography and a tetragonal cell of similar dimensions to those previously found by Dunbar and co-workers was identified.[32] The subsequent structure determination was achieved in the tetragonal space group $P4_2/mnm$. The data set collected on this crystal was not ideal, but it did yield an R_{int} value of 4.28%. Refinement of the structure resulted in a wR_2 (all data) value of 19.96% and R_1 ($I > 2\sigma(I)$) value of 6.33%. Within the structure all the TCNQ anions form stacks that extend in the *c*-direction. The TCNQ anions are inclined to the *c*-axis at an angle of 30.3(4)°. Whilst all TCNQ anions within a stack must be parallel, each TCNQ anion is disordered over two symmetry related sites. Similarly, Cu(I) centres are disordered over sites lying along the direction of the *c* axis. The disorder with both the TCNQ anion and the Cu(I) centres does not allow unambiguous identification of the network topology. A view along the direction of the TCNQ stacks is presented in Fig. 6a whilst Fig. 6b shows a single stack from side-on.

The generation of Cu(TCNQ) from the dianionic form of TCNQ, shares similarities with an approach employed in the formation of metal anilate coordination polymers.[33,34] The slow air oxidation of the tetrahydroxy aromatic form to the dianionic benzoquinone represents a favourable synthetic pathway in the formation of crystallographically usable crystals of the metal anilate polymer. It appears in such circumstances that crystal growth is promoted by the slow generation of the oxidised form of the ligand which is incorporated in the final product.

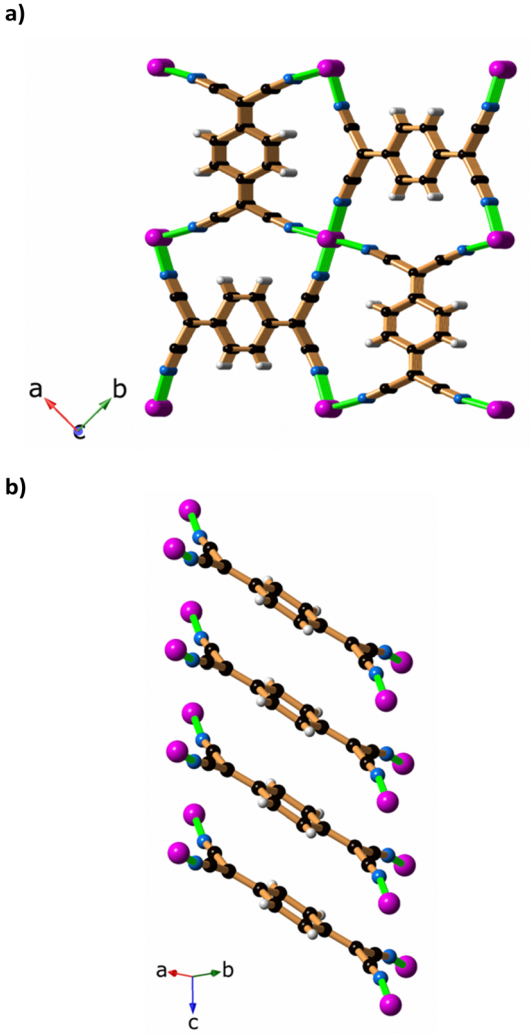

Fig. 6 The structure of Cu(TCNQ) (a) viewed along the *c*-axis and (b) showing a single stack of TCNQ ligands with a side on view; only one orientation of the TCNQ ligands is shown; similarly each Cu centre is disordered over two symmetry-related sites but only half of these sites are indicated in (b).

Conclusions

Measurement of the electrical conductivity of the 2D coordination polymer, $[Cu_2(Me_2pz)(TCNQ)]$ revealed modest semiconducting behaviour with an electrical conductivity of 9.8×10^{-8} S cm^{-1} and an activation energy of 0.43 eV. Solid-state DFT analysis reveals that the conduction bands are predominantly p-orbitals from $TCNQ^{2-}$ whilst the valence band consists largely of Me_2pz p-orbitals and thus the electrical conductivity would appear to result from a charge-transfer interaction between neighbouring $TCNQ^{2-}$ and Me_2pz ligands within infinite stacks that extend in the *a* direction. The results described in this report provide a clear example of the ability of the TCNQ in its coordinated dianionic form to participate in charge transfer interactions which result in semiconductor behaviour.

The reaction conditions that yielded $[Cu_2(TCNQ)(Me_2pz)]$ have also permitted slow air oxidation of the TCNQ dianion and in the process generated crystallographically useful crystals of Cu(TCNQ) (phase I). This result provides encouragement that other elusive metal-TCNQ materials may be generated by the slow air oxidation of the TCNQ dianion.

Conflicts of interest

There are no conflicts to declare.

Acknowledgements

The support of the Australian Research Council is gratefully acknowledged. ALS thank the Australian Government for an Australian Postgraduate Award. This research was undertaken with the assistance of resources and services from the National Computational Infrastructure (NCI), within the National Computational Merit Allocation Scheme (project fk5).

References

1 L. Sun, M. G. Campbell and M. Dinca, *Angew. Chem., Int. Ed.*, 2016, **55**, 3566–3579.
2 R. Murase, C. F. Leong and D. M. D'Alessandro, *Inorg. Chem.*, 2017, **56**, 14373–14382.
3 T. Kambe, R. Sakamoto, K. Hoshiko, K. Takada, M. Miyachi, J. H. Ryu, S. Sasaki, J. Kim, K. Nakazato, M. Takata and H. Nishihara, *J. Am. Chem. Soc.*, 2013, **135**, 2462–2465.
4 J. A. DeGayner, I. R. Jeon, L. Sun, M. Dinca and T. D. Harris, *J. Am. Chem. Soc.*, 2017, **139**, 4175–4184.
5 K. P. Goetz, D. Vermeulen, M. E. Payne, C. Kloc, L. E. McNeil and O. D. Jurchescu, *J. Mater. Chem. C*, 2014, **2**, 3065–3076.
6 M. J. Cohen, L. B. Coleman, A. F. Garito and A. J. Heeger, *Phys. Rev. B: Solid State*, 1974, **10**, 1298–1307.
7 B. F. Abrahams, T. A. Hudson and R. Robson, *Cryst. Growth Des.*, 2008, **8**, 1123–1125.
8 B. F. Abrahams, R. W. Elliott, T. A. Hudson and R. Robson, *Cryst. Growth Des.*, 2010, **10**, 2860–2862.
9 B. F. Abrahams, R. W. Elliott, T. A. Hudson and R. Robson, *CrystEngComm*, 2012, **14**, 351–354.
10 B. F. Abrahams, R. W. Elliott, T. A. Hudson and R. Robson, *Cryst. Growth Des.*, 2013, **13**, 3018–3027.
11 B. F. Abrahams, R. W. Elliott and R. Robson, *Aust. J. Chem.*, 2014, **67**, 1871–1877.
12 T. H. Le, A. Nafady, A. N. T. Vo, R. W. Elliott, T. A. Hudson, R. Robson, B. F. Abrahams, L. L. Martin and A. M. Bond, *Inorg. Chem.*, 2014, **53**, 3230–3242.
13 M. R. Saber, A. V. Prosvirin, B. F. Abrahams, R. W. Elliott, R. Robson and K. R. Dunbar, *Chem. – Eur. J.*, 2014, **20**, 7593–7597.
14 B. F. Abrahams, R. W. Elliott, T. A. Hudson, R. Robson and A. L. Sutton, *Cryst. Growth Des.*, 2015, **15**, 2437–2444.
15 B. F. Abrahams, R. W. Elliott, T. A. Hudson, R. Robson and A. L. Sutton, *CrystEngComm*, 2018, **20**, 3131–3152.

16 R. W. Elliott, A. L. Sutton, B. F. Abrahams, D. M. D'Alessandro, L. Goerigk, C. Hua, T. A. Hudson, R. Robson and K. F. White, *Inorg. Chem.*, 2021, **60**, 13658–13668.
17 T. A. Hudson and R. Robson, *Cryst. Growth Des.*, 2009, **9**, 1658–1662.
18 A. L. Sutton, B. F. Abrahams, D. M. D'Alessandro, R. W. Elliott, T. A. Hudson, R. Robson and P. M. Usov, *CrystEngComm*, 2014, **16**, 5234–5243.
19 R. A. Heintz, H. Zhao, X. Ouyang, G. Grandinetti, J. Cowen and K. R. Dunbar, *Inorg. Chem.*, 1999, **38**, 144–156.
20 J. D. Bernal, *Proc. R. Soc. London, Ser. A*, 1924, **A106**, 749.
21 T. J. Kistenmacher, T. J. Emge, A. N. Bloch and D. O. Cowan, *Acta Crystallogr., Sect. B: Struct. Crystallogr. Cryst. Chem.*, 1982, **38**, 1193–1199.
22 T. C. Umland, S. Allie, T. Kuhlmann and P. Coppens, *J. Phys. Chem.*, 1988, **92**, 6456–6460.
23 S. Matsuzaki, R. Kawata and K. Toyoda, *Solid State Commun.*, 1980, **33**, 403–405.
24 J. S. Chappell, A. N. Bloch, W. A. Bryden, M. Maxfield, T. O. Poehler and D. O. Cowan, *J. Am. Chem. Soc.*, 1981, **103**, 2442–2443.
25 S. Shimomura, N. Yanai, R. Matsuda and S. Kitagawa, *Inorg. Chem.*, 2011, **50**, 172–177.
26 T. C. Narayan, T. Miyakai, S. Seki and M. Dinca, *J. Am. Chem. Soc.*, 2012, **134**, 12932–12935.
27 S. S. Park, E. R. Hontz, L. Sun, C. H. Hendon, A. Walsh, T. Van Voorhis and M. Dinca, *J. Am. Chem. Soc.*, 2015, **137**, 1774–1777.
28 A. V. Krukau, O. A. Vydrov, A. F. Izmaylov and G. E. Scuseria, *J. Chem. Phys.*, 2006, **125**, 224106.
29 J. P. Perdew, K. Burke and M. Ernzerhof, *Phys. Rev. Lett.*, 1996, **77**, 3865–3868.
30 S. Grimme, S. Ehrlich and L. Goerigk, *J. Comput. Chem.*, 2011, **32**, 1456–1465.
31 S. Grimme, J. Antony, S. Ehrlich and H. Krieg, *J. Chem. Phys.*, 2010, **132**, 154104.
32 Crystallographic details for Cu(TCNQ), $C_{12}H_4N_4Cu$ M = 267.73, tetragonal, $a = b$ = 11.2444(6), c = 3.8703(15) Å, V = 489.3(2) Å^3, T = 100.0(1) K, Z = 2, $P4_2/mnm$, 1459 reflections measured, 295 independent reflections, R_{int} = 0.0428, wR_2 (all data) = 0.1996, R_1 ($I > 2\sigma(I)$) = 0.0633. CIF deposited with Cambridge Crystallographic Data Centre (CCDC), deposition number 2291474†.
33 B. F. Abrahams, T. A. Hudson, L. J. McCormick and R. Robson, *Cryst. Growth Des.*, 2011, **11**, 2717–2720.
34 C. J. Kingsbury, B. F. Abrahams, D. M. D'Alessandro, T. A. Hudson, R. Murase, R. Robson and K. F. White, *Cryst. Growth Des.*, 2017, **17**, 1465–1470.

